STROKE TYPE DIFFERENTIATION BY MULTI - FREQUENCY ELECTRICAL IMPEDANCE TOMOGRAPHY - A FEASIBILITY STUDY

L. Horesh *, O. Gilad *, A. Romsauerova *, A. McEwan *, S.R. Arridge ** and D.S. Holder *

* UCL/Department of Medical Physics, EIT group, London, UK
** UCL/Department of Computer Science, DOT group London, UK

l.horesh@ucl.ac.uk

Abstract: Multi-Frequency Electrical Impedance Tomography is a possible new method for differentiation of the type of acute stroke, as time difference referencing is not suitable. Local admittivity changes over frequency which simulated ischemic or haemorrhagic states were modelled in an accurate Finite Element model of the head. The resulting boundary voltages on the scalp were calculated, together with expected possible systematic errors and biases (contact impedance variations, electrode mis-location, shell thickness discrepancies and admittivity variations). Maximal absolute changes were +2% and -7% for ischemia and haemorrhage respectively, whereas changes across frequency were up to +1.7% and -2.4% for ischemia and haemorrhage correspondingly. The expected errors produced changes of about 10% in absolute values and 1% across frequency. This modelling suggests that an instrumentation accuracy of 0.01% across frequency is needed, and most discrimination for this task takes place below 100Hz and above 750kHz. To our knowledge, this is the first accurate feasibility analysis for this class of problem, and poses challenging but potentially tractable specifications for instrumentation.

Introduction

Multi - Frequency Electrical Impedance Tomography (MFEIT) is a recently developed non-invasive portable imaging technique. Acquisition is performed by injection of current at multiple frequencies through a set of scalp electrodes, and boundary voltages measurement over other sets. 3D impedance distribution maps can be reconstructed by solving the inverse admittivity problem. Biological tissue impedance changes with frequency due to the frequency-dependent behaviour of cell membranes; each tissue is characterised by a unique spectroscopic signature [1]. So far, all clinical EIT applications have been of differences over time in order to reduce modelling and instrumentation errors.

MFEIT has the potential to distinguish between haemorrhagic and ischemic brain stroke in emergency situations where CT or MRI are impractical. Tissue plasminogen activator (t-PA) is a medication that can break up blood clots and restore blood flow when administered within 3 hours of the ischemic event. Sadly, this medication is not only not applicable for haemorrhagic patients, but even likely to deteriorate their state. Recent statistics in UK shows that while about 80% of the patients suffer from ischemia, only 2.5-5% of them are classified in time and treated [2].

There are three main approaches by which this problem could be addressed: statistical analysis over the raw boundary voltages, absolute imaging or multi-frequency imaging. As it is not possible to obtain a "before" and "after" image in acute stroke, time difference imaging, which is the most robust approach, is not applicable for acute stroke. Statistical analysis of raw impedance changes ignores spatial information related to the problem. Absolute imaging does not account for inter-frequency trends and is also highly sensitive to geometrical discrepancies. Multi-frequency imaging does bear a promise of enjoying the benefits of both approaches, and yet little is known regarding the robustness of such approach.

However, before deciding upon a strategy for recovery of the internal impedance changes, it is essential to know what are the expected boundary changes due to acute stroke pathologies, and by what extent these changes are affected by variability of uncontrolled errors. The purpose of this study was to model the size of the expected changes measured with scalp electrodes during acute stroke. This was achieved using an anatomically realistic FEM mesh and three different sizes of ischemic infarction or haemorrhage. In order to assess the likelihood in reality of being able to distinguish the resulting small changes over frequency, errors due to electrode position, normal variation in tissue electrical properties, electrode contact impedance and extracerebral shell thicknesses deviations were modelled too.

Materials and Methods

Modelling: Admittivity values for normal and pathological tissues in the human head between 10Hz and 2.5MHz were obtained from the literature [3-15]. A multi layer realistic Finite Element (FE) head model of 53,336 elements, which comprised ventricles, white matter, grey matter, CSF, skull, scalp, eyes, optic nerves and internal ear canals was generated [16] (Figure 1). A complete injection-measurement protocol which covered all possible 188,790 non-reciprocal combinations has been used and a current level of 100μA was injected. Boundary voltages were calculated

ISSN: 1727-1983

for each current injection and given literature-based impedance maps, using the UCL EIT group complex impedance forward solver SuperSolver, which employs a modified version of EIDORS 3D [17]

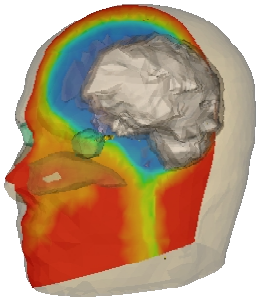

Figure 1: Multi - shell Finite Elements head model

Non-biased simulations: Simulations were conducted for normal brain, and 6 pathological cases: 3 of which were ischemic - located at the right temporal lobe comprising a volume of 4.5%, 0.7% and 0.7% of the total brain volume (Figure 2). Similarly, the other 3 cases were haemorrhagic - located at the left temporal lobe comprising volumes of 4.9%, 0.7% and 0.7% of the brain volume (Figure 3). These pathologies were designed to be of 3 levels of influence over the boundary voltages, due to the partial volume effect and proximity to the electrodes.

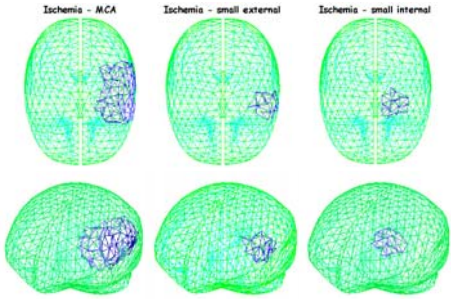

Figure 2: Brain with modeled ischemia (blue), three different cases

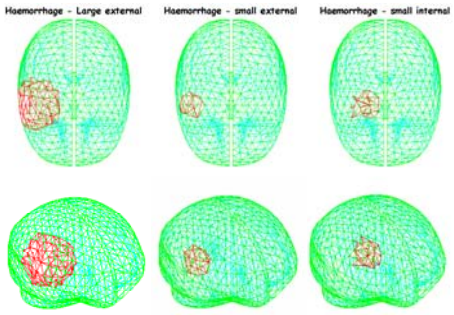

Figure 3: Brain with modeled haemorrhage (red), three different cases

Simulation of possible errors: Four types of systematic biases were introduced. Each was simulated with four increasing levels of severity: Electrode position deviation - Electrode positions were varied by 0.5-2.5 mm, which in this case comprised modifications of 5-18 surfaces out of the 37 surfaces which represent the electrodes over the mesh. Shell thickness variations - These deviated linearly from the original scale by 96% - 107% independently. Impedance variations - Conductivity and permittivity values were respectively varied by 3-9% and 1-7%. Contact impedance variations - Electrode contact impedance was varied between 0.5KΩ up to 2KΩ.from the original value of 1KΩ.

Results

Raw boundary changes: Absolute voltages – The maximal real peripheral voltage change for all pathologies occurred at the lowest modelled frequency of 10Hz. In terms of absolute voltages at 10 Hz, the peak change for ischemia compared to normal brain was +0.2 to +1.9% for the three lesions, and -0.8 to -7.1% for the haemorrhagic cases. Boundary changes decreased to +0.07% to +0.3% for ischemia (at 2.5MHz) and between -0.7% to -5.5% for haemorrhage (at 250kHz) (Figure 4). These data are for the channels with the maximum change; similar changes occurred in about 5% of channels with changes larger than half maximal.

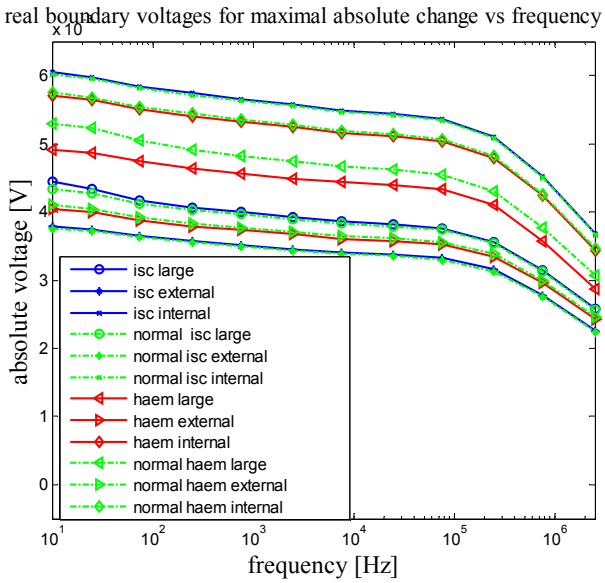

Figure 4: Absolute voltages for real maximal change vs. frequency

The baseline imaginary components of the standing voltage were smaller in magnitude, compared to the real cases, by about 10 fold. However, this component manifested larger percentage changes: +3% to +16.8% for ischemia and -3.6% to -28.5% for haemorrhage at the lower frequency band, and +0.03% to +0.3% and negative change of -0.2% to -2% correspondingly for the high frequency band (Table 1).

Relative changes with frequency - maximal changes over frequency were about 0.2% to 1.7% for ischemia and -0.3% to -2.4% for haemorrhage, and ranged

ISSN: 1727-1983

between 3%-15.5% and between -3.5%-28.5 for the imaginary part (Table 1).

Table 1: Boundary voltages percentages change for best case scenario for all pathologies

Pathology		% min real	% max real	% difference real	% min imaginary	% max imaginary	% difference imaginary
ischemia	Large external	0.2 @2.5MHz	1.9 @10Hz	1.7	0.3 @2.5MHz	16.8 @10Hz	15.5
	Small external	0.05 @2.5MHz	0.4 @10Hz	0.35	0.05 @2.5MHz	4.7 @10Hz	4.7
	Small internal	0.02 @2.5MHz	0.2 @10Hz	0.2	0.03 @2.5MHz	3 @10Hz	3
haemorrhage	Large external	-4.6 @250kHz	-7.1 @10Hz	-2.4	-0.05 @750Hz	-28.5 @10Hz	-28.5
	Small external	-1 @250kHz	-1.4 @10Hz	-0.4	-0.1 @750kHz	-4.7 @75Hz	-4.6
	Small internal	-0.5 @250kHz	-0.8 @10Hz	-0.3	-0.09 @750kHz	-3.6 @7.5kHz	-3.5

Error simulations: the simulation of errors caused changes of up to 43% for real and 76% for imaginary absolute scalp voltages. The effect over frequency was estimated using the standard deviation (Table 2 graphical example Figure 5).

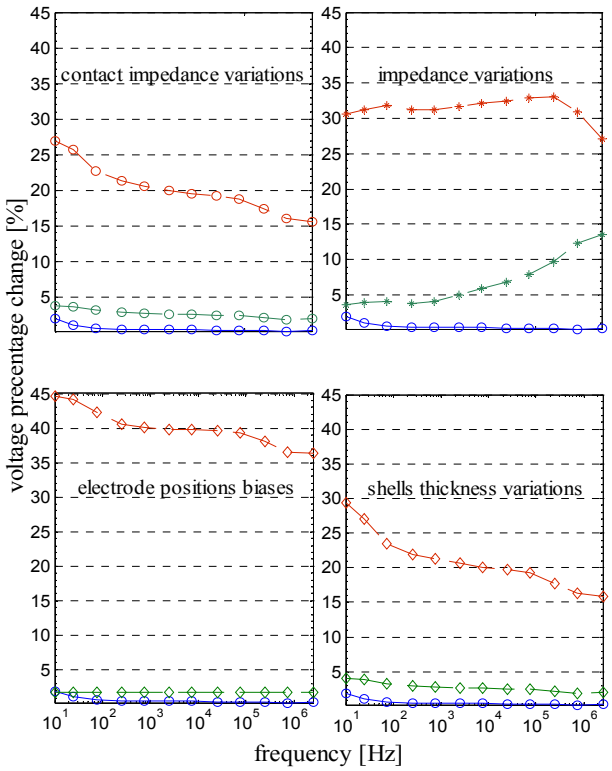

Figure 5: Effect of variations and biases with comparison to large ischemic condition, voltage percentage vs. frequency

Table 2: Change from normal brain condition introduced by the biases

	Electrodes positions		Admittivity		Shells thickness		Contact impedance	
	mean %	std %	mean %	std %	mean %	std %	mean %	std %
Real	6.3-38.6	1.6-4.2	0.8-43.7	0.05-3.2	1.2-23.5	0.6-4.2	0.8-22.2	0.6-4.4
Imaginary	1.4-41.2	0.5-14.5	11.6-19.8	13.6-24.5	6.5-80.9	2.6-53.8	4.6-76.2	1.5-42.5

Discussion

The large internal impedance contrast introduced by ischemic or haemorrhagic tissues in the brain (up to 75%-750% in local resistivity) decreases, when recorded on the scalp, to a difference between brain and lesion at the most sensitive frequency, 10 Hz, of about +2% for ischemia and -7% for haemorrhage, for the largest lesions. This represents a decrease of about 50 - 100x. The differences over frequency were clearly greatest at 10 Hz vs. higher frequencies, and were about 80% of the absolute changes.

This appears to be physiologically plausible, as the skull and the CSF introduces a shunting effect, and in addition a partial volume effect is added, therefore by the time changes are recorded on the scalp they are substantially attenuated. The most profound boundary voltage gradient trend for ischemia appears at the very low frequency band of 10Hz - 100Hz, which conforms with the central frequency for grey matter, whilst for haemorrhage additional significant trend could be found at the frequency range of 750 KHz and above. This result relates to the blood β-dispersion. We believe this is the first time these changes have been accurately modelled. This puts a severe constraint on the accuracy of instrumentation which therefore will need to be robust and accurate to fractions of a percent across frequency in order to allow imaging of these small changes.

Could better signal to noise be achieved by recording the imaginary component? Both absolute and frequency difference imaginary changes were greater than real ones by several times. However, whenever acquisition is performed over a wide range of frequencies this component of data can be derived by Kramers-Kronig relations from the real data, and therefore does not provide any additional information. Moreover, an absolute measure (rather than differential) of the imaginary component is far more difficult to record accurately than the real part, as its magnitude is smaller, thus, the SNR is expected to be lower. Overall, this is therefore unlikely to confer an advantage.

Could classification be performed reliably? In light of the above arguments, methods relying solely on the raw measurement data, such as combining bioimpedance measurements with some statistical discriminant method, are compromised by the

ISSN: 1727-1983

systematic biases, as even symmetric comparison of the right and left hemispheres will introduce an error similar to electrodes mis-location, due to the bilateral asymmetry [18]. In contrast, imaging benefits from regional localisation of changes. Absolute imaging makes use of the greatest tissue contrast, but is highly sensitive to errors in the boundary shape and electrode positioning, which probably will make it unsuitable for this application. Classification could be performed by multi-frequency reconstruction; such an approach would integrate spatial information into the solution, together with imposing spectral constraints, such as forcing the solution to have biological tissue-like spectroscopic properties. However, such a procedure requires a large-scale MFEIT inverse solution [19,20] framework, which to our knowledge is not available yet.

Conclusions

Modelling of likely errors was alarming. The introduced variation caused apparent scalp voltage changes which were larger by about an order of magnitude than the expected change due to the lesions alone. In terms of absolute imaging, it appears almost impossible that the small changes due to the lesions could be discriminated, unless other means to decrease errors were possible. For example, electrode positions would need to be measured to within mm accuracy, and initial conductivities could be inferred from MREIT or diffusion MRI. One plausible avenue might be to try and reduce the effect of errors by frequency difference imaging. However, the effect of errors seems to have an unpredicted frequency signature, which makes their elimination more difficult.

Work is in progress in our group to assess advanced machine learning methods and statistical analysis which could be used to improve discrimination, as well as improvements in hardware [21] to give greater accuracy in this demanding but potentially very valuable new application.

Acknowledgements

These are due to Andrew Tizzard of Middlesex University, London, UK for providing the accurate multi-shell head mesh.

References

[1] FOSTER K., and SCHWAN H. (1989): 'Dielectric properties of tissues and biological materials: a critical review', *Crit Rev. Biomed. Eng* 17, pp. 25-104.

[2] POWER M. (2004): 'An Update on Thrombolysis for Acute Ischaemic Stroke', *ACNR* 4.

[3] BURGER H. and VAN DONGEN R. (1960): 'Specific Electrical Resistance of Body Tissue'. *Physics in Medicine and Biology* 5, pp. 431-447.

[4] CASAS O., BRAGOS R., RIU P., ROSELL J., TRESANCHEZ M., WARREN M., RODRIGUEZ-SINOVAS A., CARRENO A., and CINCA J. (1999): 'In vivo and in situ ischemic tissue characterization using electrical impedance spectroscopy', *Ann N. Y. Acad. Sci.* 873, pp. 51-58.

[5] GABRIEL S., LAU R., and GABRIEL C. (1996): 'The dielectric properties of biological tissues: III. Parametric models for the dielectric spectrum of tissues', *Phys. Med. Biol.* 41, pp. 2271-2293.

[6] GEDDES L. and BAKER L. (1967): 'The specific resistance of biological material - a compendium of data for the biomedical engineer and physiologist', *Med. Biol. Eng 5,* pp. 271-293.

[7] LINGWOOD B., DUNSTER K., HEALY G., WARD L., and COLDITZ P. (2003): 'Cerebral impedance and neurological outcome following a mild or severe hypoxic/ischemic episode in neonatal piglets', *Brain Res.* 969, pp. 160-167.

[8] RANCK J.B., JR. (1963): 'Analysis of specific impedance of rabbit cerebral cortex', *Exp. Neurol.* 7, pp. 153-174.

[9] SCHWAN H.P. (1963): 'Electrical characteristics of tissues: a survey', *Biophysik* 1, pp. 198-208.

[10] VAN HARREVELD A., MURPHY T., and NOBEL K.W. (1963): 'Specific Impedance of rabbit's cortical tissue', *American Journal of Physiology* 2, pp. 203-205.

[11] WU X., DONG X., QIN M., FU F., WANG Y., YOU F., XIANG H., LIU R., and SHI X. (2003): 'The in vitro measurements of rabbit brain complex impedance frequency response and the equivalent circuit model', *Chinese Journal of Biomedical Engineering* 22.

[12] YAMAMOTO T. and YAMAMOTO Y. (1976): 'Electrical properties of the epidermal stratum corneum', *Med. Biol. Eng* 14, pp. 151-158.

[13] RANCK J.B., JR. (1963): 'Specific impedance of rabbit cerebral cortex', *Exp. Neurol.* 7, pp. 144-152.

[14] RANCK J.B., JR. and BEMENT S.L. (1965): 'The specific impedance of the dorsal columns of cat: an inisotropic medium', *Exp. Neurol*. 11, pp. 451-463.

[15] SEOANE F., LINDECRANTZ K., OLSSON T., KJELLMER I., FLISBERG A., and BAGENHOLM R. (2004) 'Brain Electrical Impedance at various Frequencies: the Effect of Hypoxia', *Proc. of 26th annual international conference of the IEEE Engineering in Medicine and Biology Society. San Francisco, California, 2004.*

[16] TIZZARD A., HORESH L., YERWORTH R.J., HOLDER D.S., and BAYFORD R.H. (2005): 'Generating accurate finite element meshes for the forward model of the human head in EIT', *Physiological Measurement* pp. S251-S261.

[17] POLYDORIDES N. and LIONHEART W. (2002) 'A Matlab toolkit for three-dimensional electrical impedance tomography: a contribution to the Electrical Impedance and Diffuse Optical Reconstruction Software project', *Meas. Sci. Technol* 13 (12) pp. 1871-83.

[18] TOGA W.T. and THOMPSON P.M. (2003): 'Mapping brain asymmetry', *Nature Reviews Neuroscience.*

ISSN: 1727-1983

[19] HORESH L., BAYFORD R.H., YERWORTH R.J., TIZZARD A., AHADZI G.M., and HOLDER D.S. (2004): 'Beyond the linear domain - The way forward in MFEIT image reconstruction of the human head', *Proc. of XII International Conference on Electrical Bio-Impedance, Gdansk, Poland, 2004, p.683-686.*

[20] HORESH L., SCHWEIGER M., ARRIDGE S.R., and HOLDER D.S. (2005) 'Large Scale Non-Linear 3D Reconstruction Algorithms for Electrical Impedance Tomography of the Human Brain', *Proc. of Applied Inverse Problems Conference, Royal Agricultural College, Conference Centre, UK, 2005.*

[21] MCEWAN A., YERWORTH R.J., HORESH L., and HOLDER D.S. (2005) 'Specification and calibration of a Multi-frequency MEIT system for stroke', *Proc. of 3rd European Medical and Biological Engineering Conference, Prague, Czech Republic, 2005.*

ISSN: 1727-1983